Optics Letters

Experimental comparison of E-band BDFA and Raman amplifier performance over 50 km G.652.D fiber using 30 GBaud DP-16-QAM and DP-64-QAM signals

Aleksandr Donodin,* Pratim Hazarika, Mingming Tan, Dini Pratiwi, Shabnam Noor, Ian Phillips, Paul Harper, and Wladek Forysiak

Aston Institute of Photonic Technologies, Aston University, Birmingham, UK
a.donodin@aston.ac.uk

Received 8 December 2023; revised 22 January 2024; accepted 6 February 2024; posted 6 February 2024; published 4 March 2024

We compare the performance of three optical amplifiers in the E-band: a bismuth-doped fiber amplifier (BDFA), a distributed Raman amplifier, and a discrete Raman amplifier (RA). Data transmission performance of 30 GBaud DP-16-QAM and DP-64-QAM signals transmitted over 50 km of G.652.D fiber is compared in terms of achieved signal-to-noise (SNR). In this specific case of relatively short distance, single-span transmission, the BDFA outperforms the distributed and discrete Raman amplifiers due to the impact of fiber nonlinear penalties at high input signal powers.

https://doi.org/10.1364/OL.515331

Introduction. To tackle the ever-increasing demand for data capacity and an over-burdened C-band, non-conventional technologies for increasing the capacity of wavelength-division multiplexing systems such as ultra-wideband transmission have been identified as an important, alternative, short-to-medium term approach to the long-term solution of space-division multiplexing (SDM) [1–3]. A key technology requirement to open up the spectrum of the optical fiber, and so make full use of the low loss window, is the optical amplifier for unconventional (non C+L-band) signal band amplification. To this end, the E-band can be used, especially due to the lower impact of the inter-band stimulated Raman scattering on C- and L-bands from the E-band when an appropriate guard band between them is created [4]. The E-band provides an impressive 100 nm bandwidth (15.1 THz) to work with, potentially providing capacity for more data traffic than the C- and L-bands combined. This is possible due to the availability of low water peak fibers and a diverse selection of amplification techniques [1,5].

The general benefit of all Raman amplifiers (RAs) is their ability to achieve gain in any required band given the availability of the appropriate pump wavelengths. In distributed RAs, the pump power is extended into the transmission fiber, which acts as the Raman gain fiber. Compared to discrete, or lumped, amplifiers in which gain is provided after the transmission fiber in a discrete location, the distributed RA compensates the fiber attenuation along the transmission fiber. Distributed RAs have advantages such as improved noise performance and higher signal-to-noise ratio (SNR), leading to better transmission performance [6,7]. Discrete RAs require the use of nonlinear fiber as their gain medium. RAs have no energy storage, with the conversion of pump photons to signal photons occurring on sub-picosecond timelines. This, in turn, leads to a number of noise sources that are unique to RAs [8]. The length of the gain medium of RAs is in the order of kilometers. On the other hand, there are two doped fiber amplifier techniques that provide gain in the E-band: bismuth-doped fiber amplifiers (BDFAs) [9], and neodymium-doped fiber amplifiers (NDFAs) [10]. Even though NDFAs provide good noise figure (NF), challenges with competitive electronic transitions require wavelength selective micro-structured fibers to enable efficient E-band amplification [10]. BDFAs exhibit greater gain and good NF [11,12], however, until recently the substantial gain per meter to realize relatively short amplifiers was not considered possible [12].

Our recent work has demonstrated optically amplified, E-band coherent data transmission using a distributed RA [13], a discrete RA [14], and a bismuth-doped fiber amplifier (BDFA) [15]. However, the transmission conditions (fiber length and channel count) of these experiments were quite different, and so direct comparison of the E-band amplifier performance was not possible. In this Letter, we further explore the performance of these optical amplifiers in the E-band. In the following investigation, the experimental performance of the amplifiers is compared at 1430, 1445, and 1460 nm in terms of gain, NF, effective NF, and achieved bit error ratio (BER) based on the transmission of 30 GBaud dual polarization DP-16-QAM and DP-64-QAM signals through 50 km of G.652.D fiber with no water peak.

Experimental setup. The schematics and characteristics of the three amplifiers compared in this work are presented in Figs. 1(a)–1(c). The gain and NF of the amplifiers under test is presented in Fig. 1(d). The NF and effective NF for 2 dBm launch power are shown in Fig. 1(e).

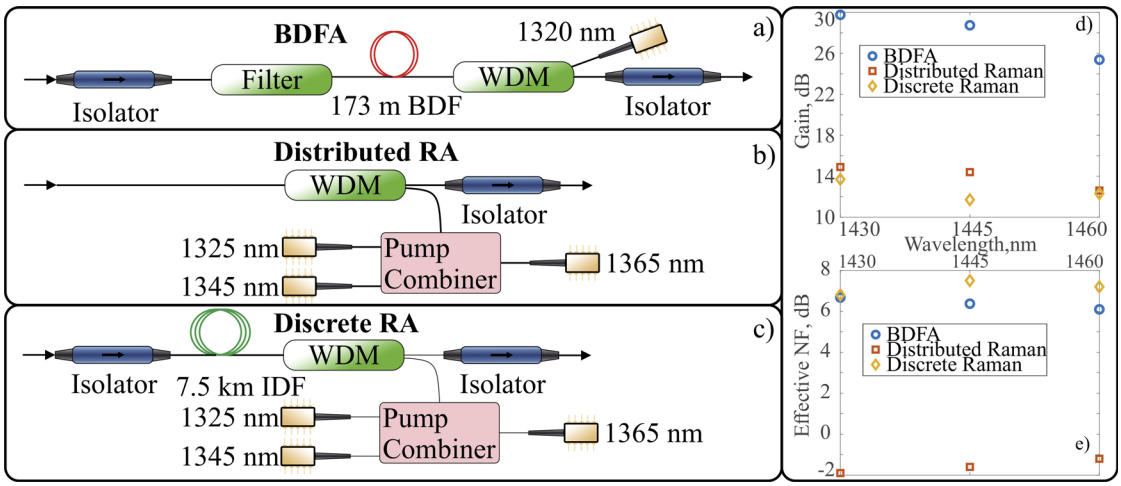

Fig. 1. (a) Schematic of the developed BDFA, (b) the distributed RA, (c) and the discrete RA; comparison of the amplifiers' characteristics: (d) gain, (e) NF.

The BDFA consists of two signal isolators and two thin-film-filter wavelength-division multiplexers (TFF-WDMs). The input filter is used to block the unabsorbed pump light. The 173-m-long active bismuth-doped fiber has a 6 μm core diameter and 125 μm cladding diameter. The refractive index difference (Δn) is around 0.007. The fiber core consists of 95 mol% SiO_2, 5 mol% GeO_2, and <0.01 at%+ of bismuth. The cutoff wavelength (λ_c) of the fiber is measured to be around 1000 nm. This amplifier design has been described previously [16], but here, we use a single pump laser diode with 460 mW at 1320 nm for backward pumping. The NF and gain of the BDFA for 2 dBm launch power (approximately −12 dBm input power) is shown in Figs. 1(d) and 1(e). The amplifier features an average NF of 6.5 dB and an average gain of 28 dB. It should be noted that the BDFA used here was designed for loss compensation of longer fiber spans; thus, its gain is significantly higher than those of the RAs. However, as the input to the receive amplifier is fixed to −20 dBm throughout the experiment, the higher gain of the BDFA under test does not impact the comparison.

The distributed RA utilizes the 50-km-long G.652.D fiber simultaneously as a transmission and amplification medium. The distributed RA comprises three pump lasers emitting radiation at 1325, 1345, and 1365 nm that are combined with a pump combiner and then a WDM filter [Fig. 1(b)]. The polarization diversity is achieved by combining two orthogonally polarized pump diodes via a polarization beam splitter (PBC) at each wavelength. The pump powers are indicated in Table 1. All the pumps are counter-propagated to the signal to minimize the effect of relative intensity noise (RIN) and nonlinear impairments in the amplifier. The amplifier pump powers are optimized to achieve flattop gain with an average of 14 dB. The average effective NF is −1.5 dB. The distributed RA exhibits minimum noise accumulation in comparison to its other counterparts due to the negative value of the effective NF.

Table 1. Pumping Wavelength and Power of Discrete and Distributed RAs

Wavelength	Distributed	Discrete
1325 nm	213 mW	261 mW
1345 nm	276 mW	111 mW
1365 nm	148 mW	267 mW

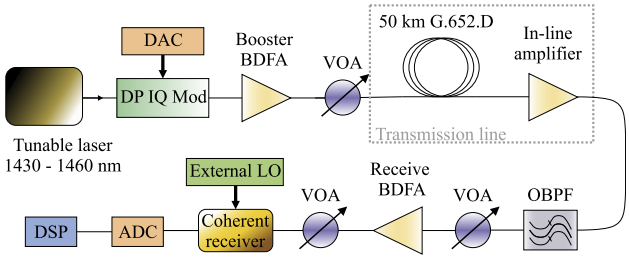

Fig. 2. Experimental setup of the transmission over 50-km-long G.652.D fiber.

The discrete RA comprises 7.5 km of inverse dispersion fiber (IDF) as a gain medium [17], backward-pumped using the same set of diode pump laser wavelengths, with pump powers as indicated in Table 1. The NF and gain of the discrete RA for 2 dBm launch signal power (approximately −12 dBm input power to the discrete RA) is shown in Fig. 1. An average NF of 7.5 dB and an average gain of 13 dB are achieved.

The setup of the E-band data transmission experiment is presented in Fig. 2. The data carrier signal is generated by a transmitter (Tx) comprising a tuneable laser (TL) operating from 1430 to 1460 nm and a DP-IQ modulator driven by a digital-to-analog converter (DAC) to generate a 30 GBaud DP-16-QAM signal. After the modulator, the signal is amplified by a second in-house BDFA designed for E- and S-band operation [9], followed by a variable optical attenuator (VOA) to control the input power to the transmission line. When transmission is performed, the signal is directed to a 50-km-long G.652.D fiber (13 dB total loss with 0.26 dB/km attenuation at 1445 nm) and then amplified by one of the three in-line amplifiers under test. The signal is then directed to an optical bandpass filter (OBPF) with 5 dB internal loss, where the data carrier is filtered from the amplified spontaneous emission (ASE).

In all transmission experiments, after filtering by the OBPF, the signal is attenuated to a fixed input power of −20 dBm with a VOA having 1 dB minimal internal loss and then amplified by the receive BDFA. The receive BDFA is based on the doped fiber

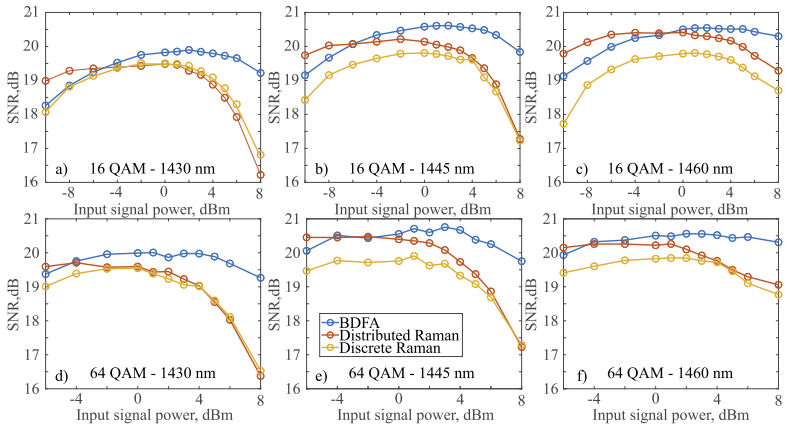

Fig. 3. Comparison of SNR for different launch powers for amplifiers under test for (a) 1430 nm, (b) 1445 nm, and (c) 1460 nm for 30 GBaud 16-QAM and for (d) 1430 nm, (e) 1445 nm, and (f) 1460 nm for 30 GBaud 64-QAM.

reported previously [16] and has a similar design to the booster amplifier. The input power to the coherent receiver is controlled by another VOA to 8 dBm. A second TL operating from 1430 to 1460 nm is used as the local oscillator (LO) for the coherent detection. Channel reception is completed by a standard set of balanced receivers and 80 GSa/s analog-to-digital converters (ADCs) and a digital signal processing (DSP) chain described previously [18].

Results. The 30 GBaud DP-16-QAM data transmission results are shown in Figs. 3(a)–3(c). Each data point is the mean signal-to-noise ratio (SNR) for the two polarizations, averaged over ten captured traces of 200,000 samples. The wavelength dependence of the SNR is recorded by tuning the wavelength of the TLs (signal and local oscillator) to 1430, 1445, and 1460 nm. This limited wavelength range was selected to avoid any impact of polarization imbalance at wavelengths below 1430 nm due to the non-optimized transceiver, as previously reported [19]. Moreover, the operation bandwidth and Raman pump wavelengths lie beyond the water peak of legacy G.652 fiber (especially pronounced for 1370–1400 nm), to which, therefore, the results might also apply. The bit error ratio (BER) measurement is conducted with each amplifier and at each wavelength for launch powers ranging from −10 to 8 dBm for 30 GBaud DP-16-QAM signals and from −6 to 8 dBm for 30 GBaud DP-64-QAM signals. The BER is then converted to the SNR using Eq. (1) from [20] and thus includes the impact of linear and nonlinear noise contributions to the SNR. We note that the underlying assumption of independent Gaussian noise distributions is limited in accuracy for single-span transmission, but nevertheless the calculated SNR is a widely adopted and useful performance metric enabling reasonable estimation and easy visualization of transmission penalties [19]. The input power to the receiver amplifier (−20 dBm) and the coherent receiver (8 dBm) remained constant throughout the experiment.

To begin with, the performance of the amplifiers is compared using a 30 GBaud 16-QAM signal [Figs. 3(a)–3(c)]. As shown in Fig. 3(a), at 1430 nm, the BDFA gives the best transmission performance overall with the optimum launch power at 2 dBm. In the linear regime, the distributed RA gives better performance from −10 to −6 dBm, due to a significantly lower NF, compared with the other two amplifiers. In the nonlinear regime, the BDFA shows the best SNR performance, whereas the distributed and discrete RAs show a similar trend. By comparison, the distributed RA suffers from higher fiber nonlinearity due to higher averaged signal power along the fiber, while the discrete RA suffers from high nonlinearity in the 7.5 km of IDF (Raman gain fiber). Balancing the impact of linear noise and nonlinearity, the distributed RA shows the lowest optimum launch power of −2 dBm, while the discrete RA and BDFA have similar optimum launch power.

The performance of the BDFA is best at 1445 nm [Fig. 3(b)]. At this wavelength, the linear regime of the BDFA extends up to a launch power of 2 dBm where the SNR is 20.6 dB. As at 1430 nm, the distributed RA again outperforms the BDFA and discrete RA in the linear regime (between −10 and −6 dBm). The optimal launch power of the distributed RA is again around −2 dBm. As at 1430 nm, the BDFA has the slowest decrease in the nonlinear regime among the three amplifiers, with the discrete and distributed RAs exhibiting similar, relatively rapidly decaying nonlinear regimes.

Finally, the results of the 30 GBaud 16-QAM transmission at 1460 nm are presented in Fig. 3(c). The performance trends at this wavelength are similar to those at 1430 and 1445 nm. However, the best performance of the distributed RA is almost identical to that of BDFA and reaches 20.4 dB SNR at the optimal launch power of 0 dBm. The BDFA still has a slightly higher SNR of 20.5 dB at the optimal launch power of 5 dBm and a flatter nonlinear regime compared to 1445 and 1430 nm. The overall performance of the discrete RA is worse than both the BDFA and the distributed RA. The performance in the nonlinear regime of both the discrete and distributed RA is better than that at 1445 and 1430 nm. The dynamic of the nonlinear regimes with wavelength is determined by the induced nonlinearity in the SMF and is discussed in detail below. Note that the wavelength dependence of the maximum SNR achieved is not only determined by the in-line amplifiers but also by the transmitter and receiver wavelength dependence through the booster and receive amplifiers (also BDFAs), the operation of the modulator, and the spectral response of the receiver photodiodes and the optical hybrid. In particular, the most limiting factor of the achieved SNR is the receive BDFA, due to low input signal power. However, this limitation is the same for all three cases with different in-line amplifiers.

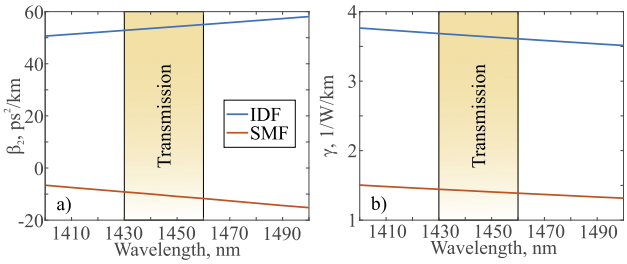

Fig. 4. Parameters of the fibers utilized in the experiment: (a) nonlinear coefficient and (b) group velocity dispersion.

The 30 GBaud DP-64-QAM results are presented in Figs. 3(d)–3(f). It should be noted that the range of the input signal power for DP-64-QAM is limited from −6 to 8 dBm. Overall, the performance trends are similar to those of DP-16-QAM. The distributed RA has the best performance at the beginning of the linear regime, which then saturates. This results in the BDFA having the best peak performance among the three amplifiers at all wavelengths. The discrete RA exhibits the worst performance, probably because the signal experiences the highest induced nonlinearity of the three cases in the IDF.

Discussion. It is to be expected that the distributed RA will outperform both the discrete RA and BDFA in terms of achievable SNR, if only NF is taken into account [Fig. 1(e)]. The slightly better performance of a distributed RA over an EDFA has been previously demonstrated in the C-band for a relatively short (75.6 km) single-span link [21]. However, here in the E-band, in terms of the achieved optimal SNR, the BDFA outperforms the distributed RA at all three tested wavelengths. This is due to the induced nonlinearity in the SMF (especially at lower wavelengths), as observed by the steep degradation of the performance of the distributed RA in the nonlinear regime (Fig. 3). The details of power distribution along the transmission fiber leading to differences in accumulated nonlinearity for different amplification schemes is important here and has been reported in [21].

In addition, we note that the difference between the optimal SNR for the BDFA and the distributed RA decreases with wavelength. This is because in SMF, the nonlinear interference (determined by the nonlinear coefficient and inversely proportional to the absolute value of dispersion) decreases with wavelength. The spectral variations of the nonlinear coefficient and group velocity dispersion for IDF and SMF are presented in Fig. 4. As seen from the figures, the impact of nonlinearity is higher at shorter wavelengths in SMF. In the discrete RA, a similar behavior can be observed and is attributable to the signal propagation in the 7.5-km-long IDF. IDF has a nonlinear coefficient 2.7 times higher than the G.652.D fiber [presented in Fig. 4(b)].

In contrast to the two RAs, in the case of the BDFA, the nonlinear penalties are predominantly caused by the signal transmission through the G.652.D fiber where the signal power is always less than in the distributed RA. In the case of the discrete RA, nonlinear penalties in the G.652.D fiber are identical to those in the BDFA case, and the additional nonlinearity arises in the 7.5-km-long IDF. When the WDM scenario is considered, the performance is expected to be worse for all three scenarios (especially in the nonlinear regime) and with a potentially greater penalty in the RA cases.

Thus, our study shows that the NF and effective NF do not provide the full picture of the potential signal performance degradation and should be compared with care, particularly in short, single-span systems operating at high power. In summary, out of the three E-band amplifiers, the BDFA shows the highest peak performance for 50 km span transmission in the range of 1430–1460 nm, followed by the distributed RA, and, finally, the discrete RA. However, the NF advantage plays a bigger role in the long-haul transmission scenario, with the distributed RA expected to outperform both the discrete RA and BDFA.

Conclusion. We have presented an experimental comparison of a bismuth-doped fiber amplifier, a discrete Raman amplifier, and a distributed Raman amplifier, in terms of signal-to-noise ratio of the received 30 GBaud DP-16-QAM and DP-64-QAM signals transmitted over 50 km of G.652.D fiber. In this specific case of relatively short distance transmission, both the G.652.D fiber in the case of the distributed Raman amplifier and the IDF in the case of the discrete Raman amplifier introduce additional nonlinear penalties, which result in the bismuth-doped fiber amplifier achieving the highest peak performance among these three amplifiers.

Funding. Engineering and Physical Sciences Research Council (EP/R035342/1, EP/V000969/1).

Disclosures. The authors declare no conflicts of interest.

Data availability. Data underlying the results presented in this paper are available upon reasonable request.

REFERENCES

1. A. Ferrari, A. Napoli, J. K. Fischer, *et al.*, J. Lightwave Technol. **38**, 4279 (2020).
2. T. Hoshida, V. Curri, L. Galdino, *et al.*, Proc. IEEE **110**, 1725 (2022).
3. J. Renaudier, A. Napoli, M. Ionescu, *et al.*, Proc. IEEE **110**, 1742 (2022).
4. N. Sambo, B. Correia, A. Napoli, *et al.*, J. Opt. Commun. Netw. **14**, 749 (2022).
5. L. Rapp and M. Eiselt, J. Lightwave Technol. **40**, 1579 (2021).
6. C. Headley and G. P. Agrawal, *Raman Amplification in Fiber Optical Communication Systems* (Academic Press, 2005).
7. J. D. Ania-Castañón, Opt. Express **12**, 4372 (2004).
8. J. Bromage, J. Lightwave Technol. **22**, 79 (2004).
9. A. Donodin, V. Dvoyrin, E. Manuylovich, *et al.*, Opt. Mater. Express **11**, 127 (2021).
10. J. W. Dawson, L. S. Kiani, P. H. Pax, *et al.*, Opt. Express **25**, 6524 (2017).
11. A. Donodin, E. Manuylovich, V. Dvoyrin, *et al.*, in *Optical Fiber Communication Conference* (Optica Publishing Group, 2023), paper Th2A–11.
12. S. Wang, Z. Zhai, A. Halder, *et al.*, Opt. Lett. **48**, 5635 (2023).
13. P. Hazarika, A. Donodin, M. Tan, *et al.*, in *Optical Fiber Communication Conference* (Optica Publishing Group, 2023), paper Th1B–7.
14. P. Hazarika, M. Tan, A. Donodin, *et al.*, Opt. Express **30**, 43118 (2022).
15. A. Donodin, M. Tan, P. Hazarika, *et al.*, Opt. Lett. **47**, 5152 (2022).
16. A. Donodin, V. Dvoyrin, E. Manuylovich, *et al.*, in *2022 European Conference on Optical Communication (ECOC)* (IEEE, 2022), pp. 1–4.
17. P. Hazarika, M. Tan, M. A. Iqbal, *et al.*, Opt. Express **30**, 43053 (2022).
18. P. Skvortcov, I. Phillips, W. Forysiak, *et al.*, IEEE Photonics Technol. Lett. **32**, 967 (2020).
19. A. Donodin, E. London, B. Correia, *et al.*, J. Lightwave Technol. **14**, 1 (2021).
20. A. Ellis, M. McCarthy, M. Al Khateeb, *et al.*, Adv. Opt. Photonics **9**, 429 (2017).
21. M. Tan, M. A. Iqbal, T. T. Nguyen, *et al.*, Sensors **21**, 6521 (2021).